

A Study of Tidal Influences in the North Water Polynya using Short Time Span Satellite Imagery

R.F. VINCENT¹ and R.F. MARSDEN²

(Received 4 September 2007; accepted in revised form 12 February 2008)

ABSTRACT. The North Water Polynya (NOW) is an area of ocean between Greenland and Ellesmere Island that does not freeze completely during the winter months. The mechanism that maintains the polynya during the Arctic winter and early spring is not precisely known, but the presence of open water is a critical factor in allowing oceanic heat to escape into the atmosphere. The northerly location of the NOW permitted the collection of an Advanced Very High Resolution Radiometer (AVHRR) image every 101 minutes for seven consecutive orbits. The unique, short time span imagery allowed thermal features of the NOW to be mapped over a tidal cycle. The combination of AVHRR imagery, Acoustic Doppler Current Profiler data, and the Composite Arctic Sea Surface Temperature Algorithm show the dynamic nature of the NOW over a tidal cycle. Both the amount and configuration of open water can change dramatically over a 12-hour period in response to tidal fluctuations. The evidence suggests that the amount of open water in the NOW during March and April is related to the velocity of the current, which in turn is influenced by the tidal cycle. The open water caused by the tide-induced movement of ice then allows oceanic heat to escape into the environment. During March and April, the considerable temperature difference between the ocean and the atmosphere at their interface results in a high incidence of ice fog near leads and open water in the NOW. The amount of ice fog observed on the satellite imagery fluctuates with the tidal cycle, suggesting that open water within the NOW is influenced by the tide in the short term.

Key words: remote sensing, polynya, Arctic, tides, oceanography, geophysics, physics, atmosphere, infrared, ice

RÉSUMÉ. La Polynie des eaux du Nord (NOW) est une zone océanique située entre le Groenland et l'île d'Ellesmere qui ne gèle pas complètement pendant les mois d'hiver. Le mécanisme qui maintient la Polynie ainsi pendant l'hiver et le début du printemps de l'Arctique n'est pas vraiment connu, mais la présence d'eau libre est un facteur critique permettant à la chaleur océanique de s'échapper dans l'atmosphère. L'emplacement nordique de la Polynie des eaux du Nord a permis de recueillir des images par radiomètre perfectionné à très haute résolution (AVHRR) aux 101 minutes pendant sept orbites consécutives. L'imagerie unique obtenue sur une courte durée a permis aux caractéristiques thermales de la Polynie des eaux du Nord d'être mappées sur un cycle des marées. Ensemble, les images captées par AVHRR, les données prélevées au moyen du profileur de courant acoustique à effet Doppler et l'algorithme composite pour les températures de surface de la mer arctique illustrent la nature dynamique de la Polynie des eaux du Nord sur un cycle des marées. La quantité et la configuration de l'eau libre peuvent changer énormément sur une période de 12 heures en raison des fluctuations attribuables aux marées. Les données recueillies laissent croire que la quantité d'eau libre dans la Polynie des eaux du Nord en mars et en avril est influencée par la vitesse du courant qui, à son tour, est influencée par le cycle des marées. Ensuite, l'eau libre découlant du mouvement de la glace provoqué par les marées permet à la chaleur océanique de s'échapper dans l'environnement. En mars et en avril, la différence considérable de température entre l'océan et l'atmosphère à leur interface entraîne une forte incidence de brouillard glacé près des chenaux et des eaux libres de la Polynie des eaux du Nord. La quantité de brouillard glacé observée sur l'imagerie par satellite fluctue en fonction du cycle des marées, ce qui laisse croire que l'eau libre dans la Polynie des eaux du Nord est influencée par la marée à court terme.

Mots clés : télédétection, Polynie, Arctique, marées, océanographie, géophysique, physique, atmosphère, infrarouge, glace

Traduit pour la revue *Arctic* par Nicole Giguère.

INTRODUCTION

The North Water Polynya (NOW), the largest polynya in the Canadian Arctic, is situated in northern Baffin Bay between Ellesmere Island to the west and Greenland to the east (see Fig. 1). Pack ice carried southward through Kane Basin becomes congested in early winter and forms a

blockage across the narrow head of Smith Sound. Newly formed ice is then swept toward the south by currents and prevailing winds (Nutt, 1969). The blockage across Smith Sound, referred to as an "ice bridge," sharply defines the northern limit of the polynya. Its southern boundary, characterized by pack ice in Baffin Bay, is more diffuse and depends on weather conditions and the time of year.

¹ Corresponding author: Department of Physics, Royal Military College of Canada, PO Box 17000, Station Forces, Kingston, Ontario K7K 7B4, Canada; Ron.Vincent@rmc.ca

² Department of Physics, Royal Military College of Canada, PO Box 17000, Station Forces, Kingston, Ontario K7K 7B4, Canada

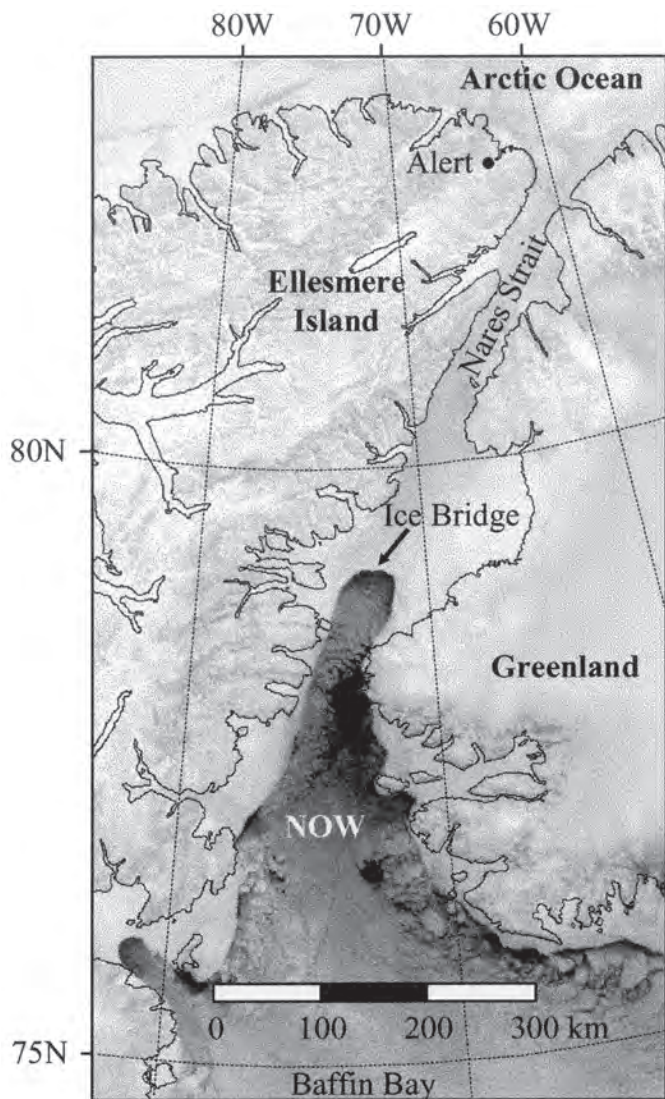


FIG. 1. A satellite infrared image of the region between Greenland and Ellesmere Island for 30 March 1998, showing the coastlines and the NOW in northern Baffin Bay. The ice bridge that forms across Smith Sound in early winter sharply defines the northern boundary of the NOW, and pack ice in Baffin Bay characterizes its southern boundary.

The NOW does not remain fully ice-free in winter, typically having 90% ice cover (Smith et al., 1990). During late March and April, the winter pack ice begins to dissipate and the polynya expands southward from Smith Sound, reaching a maximum water area of 80 000 km² in July. The polynya is indiscernible by August because Baffin Bay is ice-free, but it is re-established as ice begins to encroach into the area in September and October. Figure 2 is a series of satellite images showing the seasonal evolution of the NOW between March and July 1998.

The NOW is generally classified as a latent-heat polynya in which ice is removed from the area as quickly as it forms by winds, currents, or both. Heat loss to the atmosphere is balanced by latent heat of fusion, which is released by the continual formation of ice. An important factor in keeping the NOW open is the mechanical removal of ice from the area through a combination of

prevailing winds and surface currents (Nutt, 1969; Muench, 1971). It has been hypothesized that sensible heat from the upwelling of warm Atlantic water also contributes to polynya maintenance, particularly near the Greenland coast in winter and spring (Steffen, 1985; Barber et al., 2001).

To date, there has been little research on the influence of tides on open water in the NOW during the colder months. The greatest tidal range in the Canadian Arctic occurs in the vicinity of Kane Basin and the NOW, with M_2 tidal amplitudes reaching a maximum of 135 cm (Dunphy et al., 2005). Acoustic Doppler Current Profiler (ADCP) data obtained in the vicinity of the ice bridge show strong tidal fluctuations, which lead to current reversal just south of Kane Basin (Melling et al., 2001). This study examines the effect of tidal forces on the configuration of open water using a combination of short time span Advanced Very High-Resolution Radiometer (AVHRR) imagery and simultaneous ADCP data. Sequential AVHRR images in this study are 101 minutes apart, which allows the dynamic nature of the tides to be studied. This unique dataset, in concert with a specialized Arctic sea-surface temperature algorithm, enables an examination of open water in the NOW during the course of a tidal cycle.

DATA

In 1998 the NOW Research Network, funded by the Natural Sciences and Engineering Research Council of Canada, brought together Canadian and foreign experts in Arctic oceanography to study and model the climatic and oceanographic mechanisms involved in the formation of the NOW. As part of the NOW project, the Royal Military College of Canada installed a satellite receiving station at Canadian Forces Station Alert on the northern tip of Ellesmere Island to capture AVHRR data from National Oceanic and Atmospheric Agency (NOAA) polar orbiting satellites. The northerly latitude of the study area makes this a unique dataset. Generally, the polynya was in view for seven consecutive passages between 1100 and 2300 UTC daily (all times are given as UTC). The time between images was approximately 101 minutes. A total of 1440 NOAA-12 images were acquired between 10 March and 2 August, of which 317 were sufficiently cloud-free to be retained for subsequent analysis.

The Composite Arctic Sea Surface Temperature Algorithm (CASSTA) was applied to the imagery, which allowed a thermal mapping of open water and marginal ice zones within the NOW (Vincent, 2006; Vincent et al., 2008a). CASSTA also permitted the identification of probable ice fog, a low-lying absorptive feature that could not be detected visually (Vincent, 2006; Vincent et al., 2008b). The application of CASSTA was limited to those days for which there were at least four cloud-free images, a total of 181 images on 32 days between 11 March and 27 July.

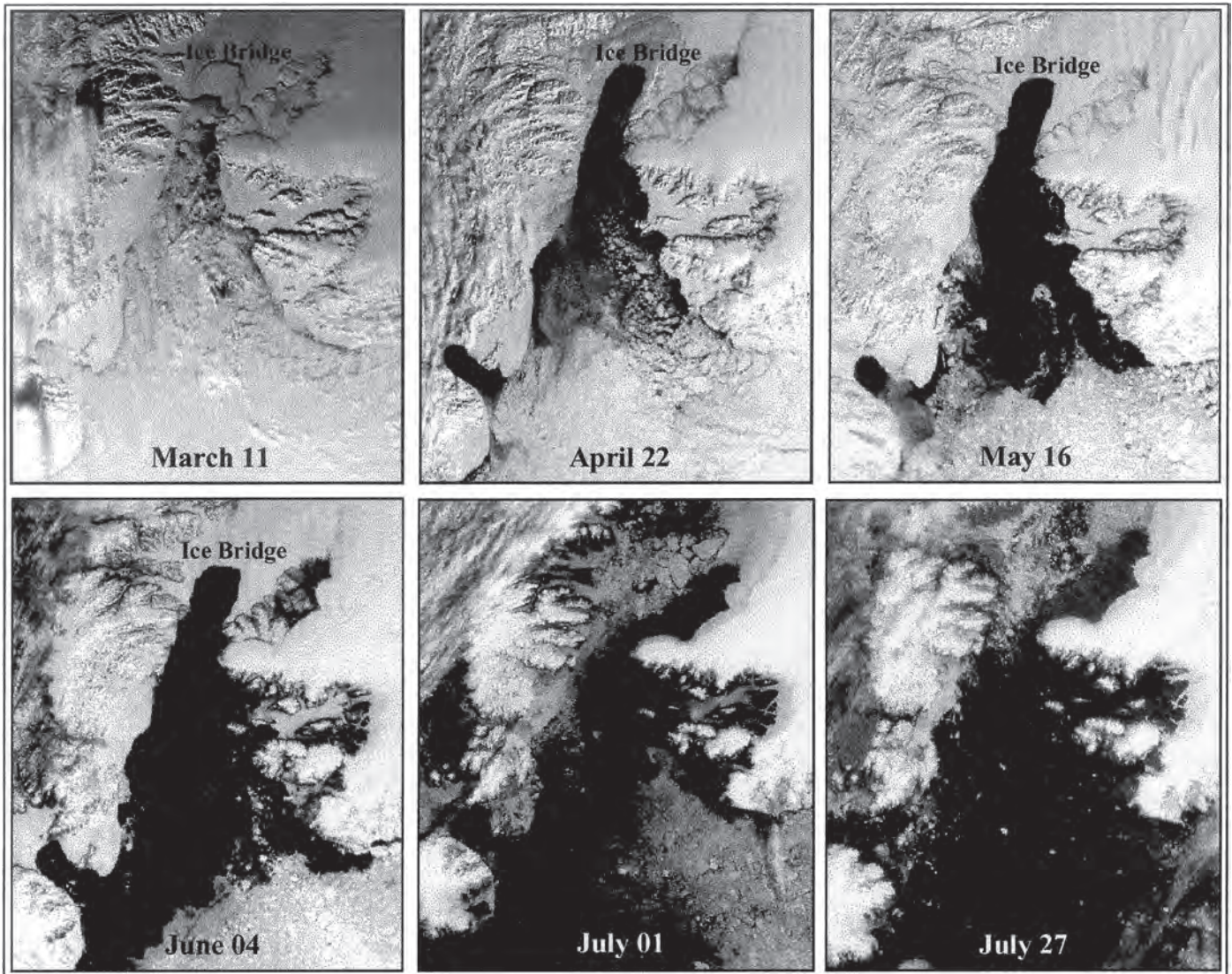


FIG. 2. The seasonal evolution of the NOW is shown in this sequence of satellite images taken from March to July 1998. The ice in the polynya diminishes in April and May. In June the ice bridge breaks up, and the polynya is no longer defined. Ice floes continue to enter the polynya via Nares Strait and move southward during the summer.

In conjunction with the sequential AVHRR imagery, we used ADCP data in the analysis, specifically to ascertain the direction and relative strength of the tide. Simultaneous ADCP and AVHRR data were available between 11 March and 18 July. ADCP N2 was located southwest of the ice bridge, where the tidal cycle caused periodic switching of the current from north to south at approximately 12-hour intervals (Melling et al., 2001). The depth of measurement at ADCP N2 differed by as much as 140 m from the nominal instrument depth of 110 m because the sensor was pulled down by strong currents. Overall, the northerly component at this sensor was stronger because of the outflow from Nares Strait, but the magnitude of the current decreased and often reversed direction during the tidal cycle. Figure 3 illustrates the variability of ADCP N2 resulting from strong tidal fluctuations. Although the depth at N2 was not reliable, it proved useful in determining the direction and relative strength of the tide, which could then

be related to surface phenomena observed in the NOW. Figure 4 shows the location of ADCP N2, as well as geographical points of interest in the NOW region. The ADCP data at the N2 location were used for the tidal analysis because N2 was near the tidal study area.

The current-magnitude readings in this study are from bin 3, which is 16 m from the sensor. This location represents a depth of 94 m, tidal pull-down of the N2 sensor notwithstanding. Bin 3 was chosen for the study because the data were assessed as 100% good at this depth for N2 (Melling et al., 2001). Bin 3 also appeared to be a reasonable indicator of current speed in the upper water column. In this analysis, the absolute velocity of the current is less important than trends of strength and direction. Therefore, the current data shown on the ADCP charts will be used to infer general conditions on the surface with respect to current speed and direction.

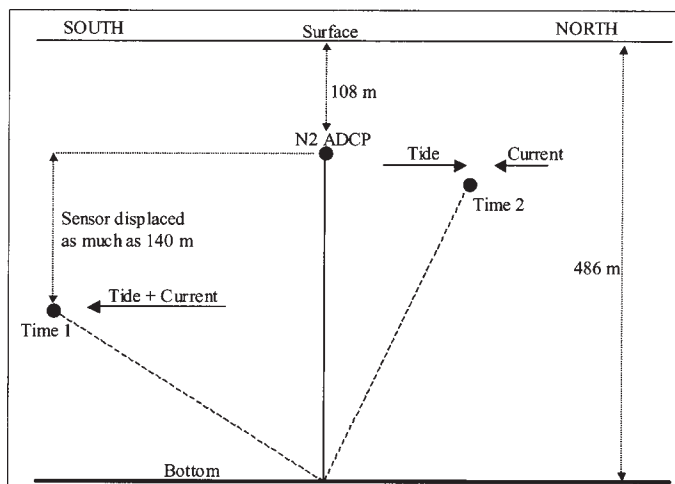


FIG. 3. The ADCP sensor at site N2 experienced pull-down due to strong tidal fluctuations. Deviation from the nominal depth was more pronounced when the tide coincided with the southward-flowing current emerging from Nares Strait. Pull-down during peak tides was as much as 140 m. When the tide counteracted the current, there was generally a reversal in flow, although this was not always the case.

TIDAL ANALYSIS

Satellite images in this study show that the NOW opens from a relatively small kernel of open water just south of Cape Alexander, which persists during March and April despite average monthly temperatures of approximately -30°C and -17°C , respectively (Environment Canada, 2007). The perimeter of this area is close to the 200 m isobath line, and is the focus for the tidal analysis (see Fig. 4). The area of open water in the NOW is less than 1000 km² in early March, but increases to over 2000 km² by mid April and expands to 15 000 km² by early May, even though daily temperatures are still below freezing. Toward the end of May, the polynya opens rapidly as the pack ice in Baffin Bay retreats southward. In June, the ice bridge dissolves, allowing southward-moving ice to transit freely through Nares Strait. By August, the NOW is indiscernible because of the ice-free condition of Baffin Bay, but it is re-established within a few months as ice encroaches on the region once again.

The open water south of Cape Alexander results from the mechanical removal of ice by wind and current (Muench, 1971). This site is a potential area of sensible heat produced by the upwelling of warm West Greenland Current waters (Steffen, 1985; Barber et al., 2001), although no warm water cells were detected during this study. The dominant north wind suggests that an offshore transport of surface water and hence upwelling on the Greenland shore is possible. However, if upwelling occurred during the time frame of the study, it was below the thermal and spatial resolution of the AVHRR sensor. In the development of CASSTA, it was discovered that standard ice and sea surface temperature algorithms produce false warm anomalies in regions of ice fog, which resemble open water on AVHRR imagery

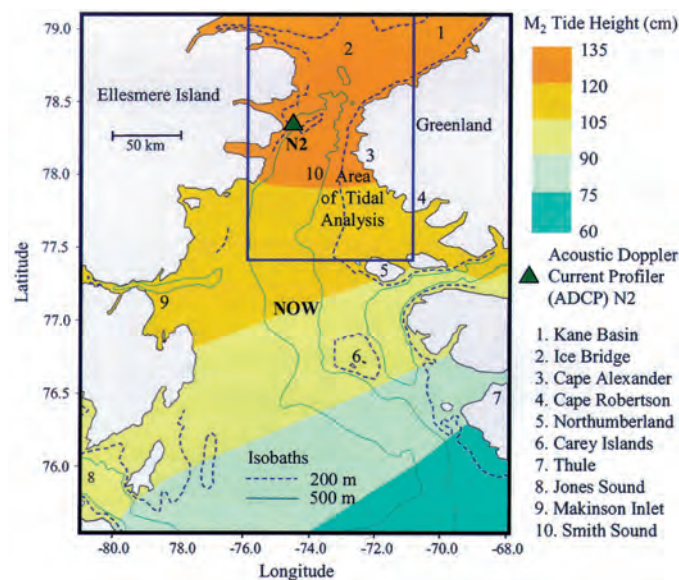


FIG. 4. A map of the NOW, showing typical M_2 tide heights (adapted from Dunphy et al., 2005) and points of interest in the NOW region, including the study area and the location of ADCP N2. The blue box outlines the area covered by AVHRR sequences in Figures 5 and 6.

because of the spectral properties of ice crystals (Vincent et al., 2008a, b).

Sequences of CASSTA imagery demonstrated that in the short term, the areas of open water change constantly in both shape and size. When the imagery is put in context with simultaneous ADCP data, it becomes apparent that the dynamic nature of the open water is, in part, a function of tidal fluctuations. Unlike the prevailing winds and ocean currents, which generally transport ice southward (Ito, 1982), the tide causes bidirectional movement of ice. During strong tidal periods, ice floes can move northward then southward depending on the tidal direction. These tidal fluctuations may also allow the mobilization of floes, creating areas of open water. On a larger scale, the periodic divergence and convergence of the pack ice in the main body of the NOW may create cracks in the ice that allow oceanic heat to escape.

In the colder months, the movement of ice over a tidal cycle directly influences the amount and configuration of open water in the polynya over the short term. The combination of concurrent ADCP and AVHRR data, in concert with the CASSTA algorithm, allowed a quantitative assessment of open water in the NOW during the course of a semidiurnal tidal cycle. March and April were the only months in which this type of analysis could be conducted because the NOW is relatively ice-free by early May. This selection process left a total of nine days, five in March and four in April, that were appropriate for study. Sequences of images for 30 March and 24 April were subsequently chosen for the analysis since those were relatively clear of ice fog, permitting an accurate calculation of open water. The images for those days also coincided with current reversals due to tides, a situation that was conducive to the study of how tidal forces influence ice movement.

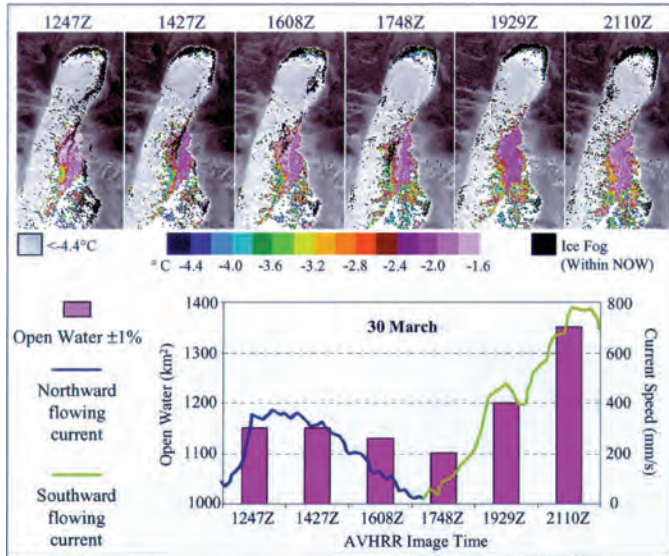


FIG. 5. Six thermal satellite images of the study area over 8.4 hours on 30 March. On the CASSTA images, open water appears as shades of purple, which represent temperatures near the freezing point of seawater (-1.8°C). Current velocities at ADCP N2 are displayed below the CASSTA images, in conjunction with the area of open water calculated for each image. Together these data indicate a bidirectional movement of ice due to tides, which is unlike the general southward transport of ice by prevailing winds and ocean currents.

30 March

Figure 5 shows six consecutive CASSTA images taken between 1247 and 2110 on 30 March. Simultaneous ADCP data are also shown in conjunction with the amount of open water determined for each scene. During this 8.4-hour span, the current velocity changed from northward at 300 mm/s to southward at 700 mm/s, with the reversal occurring between the 1608 and 1748 images. The prevailing current in this region is toward the south through Nares Strait, so the southward movement of water is stronger than the northward movement for any given tidal cycle at N2. In this case, the CASSTA images capture a strong transition in the tidal flow. During the tidal changeover, the amount of open water decreases by 2.5% (28 km²) between 1608 and 1748 and then increases by 22.5% (248 km²) from 1748 to 2110. Figure 5 also illustrates the correlation between the amount of open water and the strength of the current, which is changing in response to the tide. The minimum amount of open water occurs when the current speed approaches zero during the intertidal period. As the current accelerates in a southward direction from 0 to 700 mm/s between 1748 and 2110, there is a corresponding increase in the area of open water, which expands 7 km southward during this time.

Wind may also be a factor in moving ice. No meteorological data were available in the NOW for this time period, but adjacent areas reported calm conditions. Grise Fiord (76.4°N , 82.9°W) to the west recorded a wind speed of zero during the time frame of the analysis, while both Alert (82.5°N , 62.3°W) to the north and Pond Inlet (72.7°N , 78.0°W) to the southwest recorded consistent

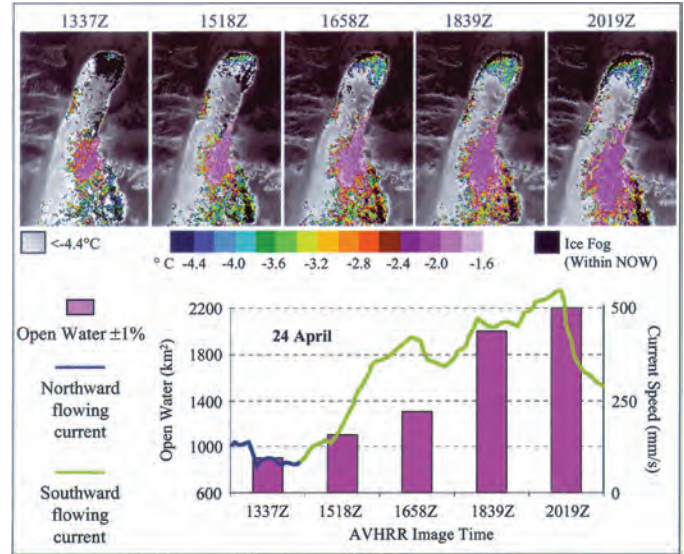


FIG. 6. Five CASSTA images of the study area over a 6.7-hour interval on 24 April. Representations for open water and current velocity are the same as in Figure 5. In this case, the intertidal period occurs at the beginning of the sequence, coinciding with the minimum amount of open water observed for the set.

north-northeast winds with an average speed of only 2 kts (Environment Canada, 2007). Historically, winds in the study area blow from the north-northeast (Barber et al., 2001), which matches the observations in Alert and Pond Inlet. The unidirectional nature of both recently recorded and historical winds in the region does not correlate well with the north-south movement of floes observed in the NOW during this period, indicating that the ice dynamics are likely the result of current changes due to tides.

24 April

Figure 6 shows five consecutive CASSTA images between 1337 and 2019. Simultaneous ADCP data are also shown in conjunction with the amount of open water determined for each scene. This sequence of images is similar to the one from 30 March (Fig. 5), except that the area of open water has increased overall and the ice is showing a warming trend. In Figure 6, the ADCP data show a weak, northward-moving current (75 mm/s) in the first image, which then changes to a southward movement of water that increases to 500 mm/s within five hours. As on 30 March, the minimum amount of open water occurs when the current speed is lowest. As the current accelerates during this 6.7-hour span, the open water in the study area increases from 900 km² to 2200 km², representing a 244% increase in the area available to exchange oceanic heat with the atmosphere. Between 1518 and 1839, as the southward current strengthens from 100 mm/s to 450 mm/s, the open water expands approximately 20 km in the same direction and increases in area by 800 km². If the polynya continued to expand at this rate, the NOW would be free of ice within seven days. The rate of open water expansion

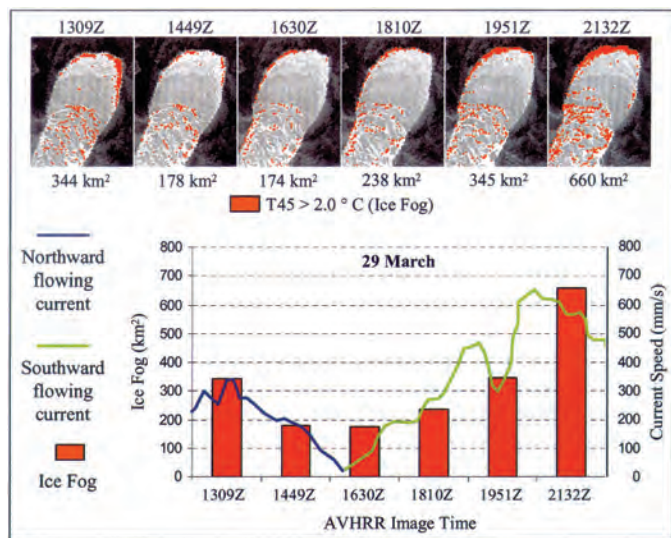


FIG. 7. Ice fog ($T_{45} > 2^{\circ}\text{C}$) south of the ice bridge is shown in relation to ADCP N2 data for 29 March. The chart is a graphical representation of the amount of ice fog in the scene in relation to current magnitude.

decreases between 1839 and 2019 as the next tidal cycle causes the flow to diminish.

Wind data were recorded by the Canadian Coast Guard Ship (CCGS) *Pierre Radisson*, which was in the NOW (76°N , 74°W) on 24 April. Between 1300 and 2100, the wind was relatively steady from the northwest, with an average speed of 12.9 kts. In this case, the wind may have assisted in pushing ice southward, although the expansion of open water in the latter images of Figure 6 is toward the southwest and not toward the southeast, as might be expected from a northwest wind. Additionally, the constant wind speed does not correlate with the changing rates of expansion, suggesting that current fluctuation in response to tidal forces is the main driving mechanism of open water expansion.

TIDES AND THE OCCURRENCE OF ICE FOG

The NOAA-12 AVHRR has five spectral channels: two visible channels and three that are capable of detecting emitted infrared from the surface. Channel 4 ($10.3\ \mu\text{m}$ to $11.3\ \mu\text{m}$) and Channel 5 ($11.5\ \mu\text{m}$ to $12.5\ \mu\text{m}$) are the primary channels used to determine sea surface temperature. In the development of CASSTA, it was found that regions in which the differential between Channel 4 and Channel 5 (T_{45}) exceeded 2°C were areas covered by ice fog that cloaked the surface temperature (Vincent, 2006; Vincent et al., 2008b). Because of the considerable temperature difference at the ocean-atmosphere interface during March and April, there is a high incidence of ice fog in the vicinity of leads and open water in the NOW. During those months ice fog commonly obscured the surface temperature of the NOW in areas where there appeared to be open water on the visible imagery. The CASSTA imagery frequently showed ice fog along the western

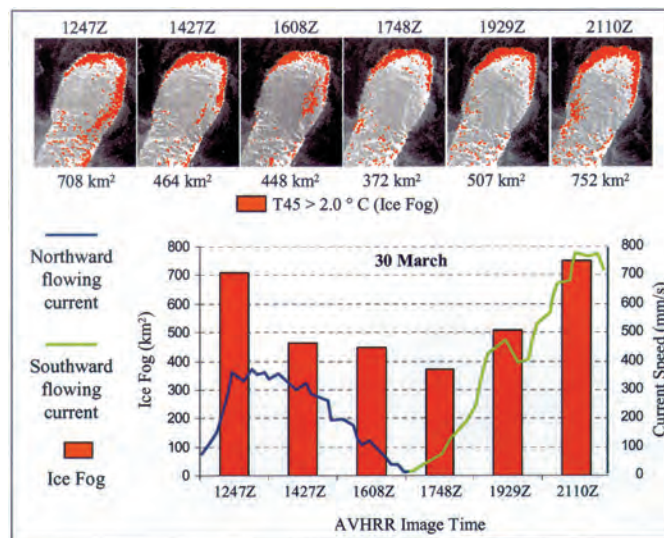


FIG. 8. Ice fog ($T_{45} > 2^{\circ}\text{C}$) south of the ice bridge is shown in relation to ADCP N2 data for 30 March. The chart is a graphical representation of the amount of ice fog in the scene in relation to current magnitude.

Greenland coast, south of the Carey Islands, Makinson Inlet, Jones Sound, and numerous leads and openings in the pack ice. The most persistent area of ice fog occurred just south of the ice bridge, appearing to some extent on all the available imagery between 11 March and 12 May. By 26 May, the phenomenon was no longer observed anywhere in the NOW. Although the water was still near freezing (-1.8°C) on this date, meteorological data from the CCGS *Pierre Radisson* indicate that the ambient temperature in the region had risen to a daily average of -1.6°C .

The CASSTA imagery suggests that the amount of ice fog is related to tidal forces. This is particularly true in the vicinity of the ice bridge, where large tidal influences produce the most pronounced current fluctuations. Figures 7 and 8 show the incidence of ice fog ($T_{45} > 2^{\circ}$) near the ice bridge in relation to ADCP N2 data for 29 March and 30 March, respectively. The relationship between ice fog coverage and current strength is also shown graphically below the images. On both dates, there is a current reversal from north to south that coincides with the AVHRR imagery. During the low flow period on these days, as the current changes direction, there is less ice fog. This low is followed by a rapid increase in ice fog as the southward-moving current accelerates to more than 500 mm/s on both days. On 30 March, more ice fog occurs in the area than on 29 March and corresponds to currents that are 100 m/s stronger in both directions than on 29 March.

Lindsay and Rothrock (1993) reported that the presence of ice fog, especially in the vicinity of leads, was the major source of errors in calculating surface temperature of sea ice. Figure 9 shows areas of ice fog superimposed on the Channel 4 (T_4) thermal image of the area. Lighter areas are warmer, while darker areas indicate colder T_4 values. The Channel 4 images in Figure 9 indicate that many of the leads within the polynya are associated with ice fog. As the current accelerates southward, ice fog

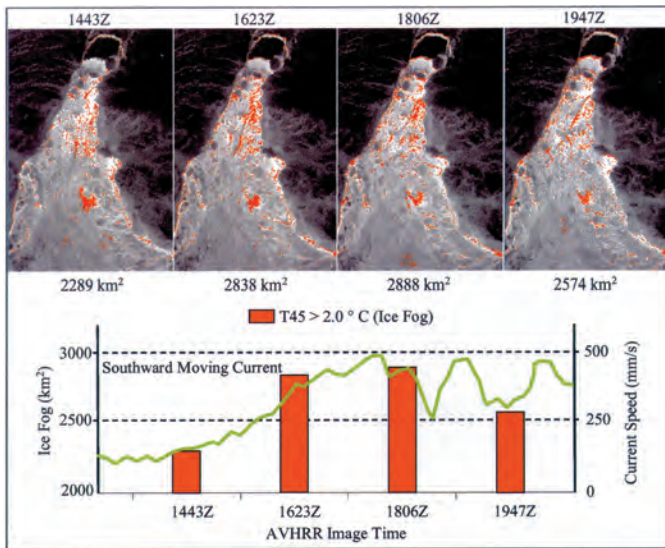


FIG. 9. The occurrence of ice fog ($T_{45} > 2^{\circ}\text{C}$) in the NOW is shown in relation to N2 ADCP data for 11 March. There is an increase in the amount of ice fog in the leads as the southward-moving current increases during the tidal period.

increases, suggesting a corresponding increase in open water. Interestingly, ice fog also builds with strengthening current around the large floe that has broken off from the ice bridge. The floes just south of the ice bridge move several kilometres southward in the five-hour span of this sequence.

SUMMARY

The NOW is generally classified as a latent-heat polynya in which ice is removed from the area by winds, currents, or both as quickly as it forms. Heat loss to the atmosphere is balanced by latent heat of fusion, which is released by the continual formation of ice. A key factor keeping the NOW open is the removal of ice from the area through a combination of prevailing winds and surface currents (Nutt, 1969; Muench, 1971). Although this ice removal is southward over the long term, this study indicates that ice moves both southward and northward in response to tidal fluctuations. The highest tides in the Canadian Arctic are found in the vicinity of the NOW (Dunphy et al., 2005). Acoustic Doppler Current Profiler (ADCP) data obtained in Smith Sound support the tidal models for the region, showing strong tidal fluctuations that lead to current reversal of the Nares Strait outflow (Melling et al., 2001). This movement of ice over a tidal cycle is related to the amount of open water in the polynya over the short term.

The combination of short time span AVHRR imagery, ADCP data, and the CASSTA algorithm illustrate the dynamic nature of the NOW over a tidal cycle. Both the amount and the configuration of open water can change dramatically over a 12-hour period in response to tidal fluctuations. The evidence suggests that the amount of open water in the NOW during the colder months is related to current velocity, which in turn is influenced by the tidal

cycle. The open water caused by the tide-induced movement of ice then allows oceanic heat to escape into the environment. The considerable temperature difference at the ocean-atmosphere interface during March and April produces a high incidence of ice fog in the vicinity of leads and open water in the NOW. The amount of ice fog observed on the satellite imagery fluctuated with the tidal cycle, suggesting that in the short term, the amount of open water within the NOW was being dictated by the tide.

The use of sequential AVHRR images separated by 101 minutes, ADCP data, and a specialized Arctic sea surface temperature algorithm allowed a unique analysis of how the NOW responds to tidal fluctuations in the March and April time frame. The amount of open water and the configuration of ice are variable, depending on the magnitude of the tide. The result is a polynya that is highly dynamic with respect to open water and subsequent heat exchange with the atmosphere over a 12-hour tidal cycle.

ACKNOWLEDGEMENT

The authors were supported by NSERC Discovery Grant 250059-2002.

REFERENCES

- BARBER, D.G., HANSIAK, J.M., CHAN, W., and PIWOWAR, J. 2001. Sea ice and meteorological conditions in northern Baffin Bay and the North Water Polynya between 1979 and 1996. *Atmosphere-Ocean* 39(3):343–359.
- DUNPHY, M., DUPONT, F., HANNAH, C.G., and GREENBERG, D. 2005. Validation of a modelling system for tides in the Canadian Arctic Archipelago. *Canadian Technical Report of Hydrography and Ocean Sciences* 243. 70 p.
- ENVIRONMENT CANADA. 2007. Hourly data reports, climate data online, Nunavut. www.climate.weatheroffice.ec.gc.ca/climateData/canada_e.html.
- ITO, H. 1982. Wind through a channel: Surface and wind measurements in Smith Sound and Jones Sound in northern Baffin Bay. *Journal of Applied Meteorology* 21:1053–1062.
- LINDSAY, R.W., and ROTHROCK, D.A. 1993. The calculation of surface temperature and albedo of Arctic sea ice from AVHRR. *Annals of Glaciology* 17:391–397.
- MELLING, H., GRATTON, Y., and INGRAM, G. 2001. Ocean circulation within the North Water Polynya of Baffin Bay. *Atmosphere-Ocean* 39(3):301–325.
- MUENCH, R.D. 1971. The physical oceanography of the northern Baffin Bay region. Montreal and Washington, D.C.: Baffin Bay North Water Project, Arctic Institute of North America. 150 p.
- NUTT, D.C. 1969. The North Water of Baffin Bay. *Polar Notes Occasional Publication* 9. Hanover, New Hampshire: Stefansson Collection, Dartmouth College.
- SMITH, S.D., MUENCH, R.D., and PEASE, C.H. 1990. Polynyas and leads: An overview of physical processes and environment. *Journal of Geophysical Research* 95(C6):9461–9479.

- STEFFEN, K. 1985. Warm water cells in the North Water, northern Baffin Bay, during winter. *Journal of Geophysical Research* 90(C12):9129–9136.
- VINCENT, R.F. 2006. A radiometric study of the North Water Polynya using the Composite Arctic Sea Surface Temperature Algorithm: T45, tides and the spring melt. PhD thesis, Royal Military College of Ontario, Kingston, Ontario. 255 p.
- VINCENT, R.F., MARSDEN, R.F., MINNETT, P.J., CREBER, K.A.M., and BUCKLEY, J.R. 2008a. Arctic waters and marginal ice zones: A composite Arctic sea surface temperature algorithm using satellite thermal data. *Journal of Geophysical Research* 113, C04021, doi:10.1029/2007JC004353.
- VINCENT, R.F., MARSDEN, R.F., MINNETT, P.J., and BUCKLEY, J.R. 2008b. Arctic waters and marginal ice zones: 2. An investigation of Arctic atmospheric infrared absorption for advanced very high resolution radiometer sea surface temperature estimates. *Journal of Geophysical Research* 113, C08044, doi:10.1029/2007JC004354.